International Journal of Computer Information Systems and Industrial Management Applications
ISSN 2150-7988 Volume 18(11s) 2026 pp. 414-429
https://doi.org/10.70917/ijcisim-2026-3763
Article

Design and Performance Analysis of a Fractal Micro-strip Patch Antenna with Defected Ground Structure

Manjunath K[1], Pavithra A C[2], Asha M[3]

[1]Department of ECE, ATMECE, Mysuru, India
manjunathatme@gmail.com
[2]Department of CSD, ATMECE, Mysuru, India
pavithraac26@gmail.com
[3]Department of ECE, GSSSIETW, Mysuru, India
asha.m@gsss.edu.in

Abstract: Microstrip Patch Antennas (MPA) are very popular in wireless communication systems due to their compactness, low profile, light weight, and ease of fabrication. The conventional microstrip antennas, however, have drawbacks like limited bandwidth, low gain, and single-frequency operation, which limit their applications in satellite communication, radar, and other advanced wireless systems. For the above problems, the design and analysis of a fractal patch array antenna with Defected Ground Structure (DGS) techniques to improve the performance of the antenna, and the design of a fractal antenna are discussed. The fractal geometries, such as the Sierpinski Triangle and Koch Curve, are used due to their self-similarity and space-filling properties, allowing for compact multiband and wideband antenna operation. The DGS is used to redistribute the ground-plane current distribution, which, in turn, improves the impedance matching, lowers the surface-wave losses, and increases the radiation efficiency. The proposed antenna is designed and simulated using the electromagnetic simulation software ANSYS HFSS. The important parameters that are required for the antennae like return loss, Voltage Standing Wave Ratio (VSWR), radiation pattern, gain and bandwidth are analyzed. The optimized antenna has a minimum return loss (S11) of about -55 dB at 8.6 GHz, a peak gain of 8.4 dBi, a VSWR of 1.02, and an impedance bandwidth of nearly 4.5 GHz in the -20 GHz operating frequency range. The proposed antenna applies to the modern multi-band wireless, radar, and satellite communication systems.

Keywords: Antenna, Microstrip, Defected Ground Structures (DGS), ANSYS, Sierpinski Triangle, Koch Curve Bandwidth, Fractal Patch Array

1. Introduction

Wireless communication systems have experienced tremendous growth in recent years, resulting from the growing demand for WC, such as satellite systems, IoT devices, radar discovery, Wi-Fi, WiMAX, WBAN, and new 5G/6G mobile communication technologies [1-3]. Modern applications demand compact, lightweight, and high-performance antennas with a capability of multiband operation, high data transmission rates, and reliable communication in a multipath wireless environment [4]. The most frequently used type of antenna is the MPA for its Interoperability with planar circuitry, small footprint, inexpensive manufacture, and ease of integrating [5]. Although these advantages exist, the conventional microstrip antennas suffer from several disadvantages that are not suitable for the advanced wireless systems such as narrow bandwidth, low gain, low radiation efficiency and single band operation [6].

Research efforts have been directed at developing techniques to reduce the size of the antenna and increase its bandwidth through the use of novel geometrical and electromagnetic solutions to overcome these challenges [7]. Slots, meanderings, folding, and ground plane engineering have been explored and utilized intensively to enhance the antenna features with compact dimensions [8, 9]. In particular, fractal-based antenna configurations have been the object of great interest due to their self-similarity and space-filling characteristics that allow for compact size reduction and multiband operations [10]. Several geometric arrangements are known to improve the resonant properties, impedance matching, and frequency flexibility for current wireless applications [11].

Another interesting technique is the use of defective ground structures in which deliberate faults are introduced into the ground-level layer that determines how surface current is distributed [12]. The structures not only extend the impedance bandwidth but also lower the surface-wave losses, suppress mutual coupling, and boost the gain and radiation efficiency of the antennas [13]. Various defect forms, including rectangular, circular, dumbbell, spiral, U-shaped, and hexagonal, have been investigated for microwave and antenna applications [14]. Recent studies also show that the use of fractal configurations combined with defected ground techniques can significantly enhance the multiband behavior, the bandwidth, and the overall antenna efficiency [15].

While challenges like maintaining radiation efficiency, going down to miniaturization, keeping the performance stable for multi-bands, reducing the level of cross-polarization, and minimizing the inaccuracies in the fabrication process remain [16]. Furthermore, the differences between simulation and actual implementation remain a problem for antenna optimization so far [17]. There are various advanced numerical methods, such as FEM, FDTD, and MoM, that are now used to obtain accurate electromagnetic analysis and parametric optimization [18]. Thus, design concepts for integrated antennas are investigated with a view to designing a compact, high-gain, wideband, and efficient antenna system, which meets the demands of modern wireless communication [19]. The current research involves the development of a compact multi-band microstrip fractal antenna with ST, KC, and DGS techniques for increasing bandwidth, gain, impedance matching, and wireless communication efficiency for WLAN, WiMAX, IoT, and satellite systems.

1.1 Key Contributions

- Designed a compact multiband MPA with Sierpinski–Koch fractal geometry and DGS for improving the wireless performance.
- Improved antenna properties, including good impedance matching, gain, wideband, and strong multiband resonance properties.
- Optimized defect engineering of the ground plane, which showed good defect reduction of surface wave losses and good radiation efficiency.
- Simulated a model of an antenna in full scale using Matrix Laboratory (MATLAB), optimized it by systematic fractal iteration, and parametric optimization.
- Proposed some ideas on the design of the antenna that can be scalable for modern applications like communication, radar, IoT, satellite systems, etc.

In Section 2, the literature survey on fractal and microstrip antenna design is presented. The proposed antenna design method is explained in Section 3, with the fractal geometry and DGS integration. The results of the

simulation and performance analysis of the developed antenna are discussed in Section 4. Finally, Section 5 concludes the research by summarizing the important findings, limitations, and future research possibilities.

2. Literature Review

In the literature, the progress of 5G, RF harvesting, MIMO, and biomedical imaging based on fractal and microstrip antennas is highlighted, with some limitations such as moderate gain, losses, narrowband operation, and the lack of real-time deployment analysis. The microwave imaging of bio-phantoms using microwave images computed from the in-silico/in-vitro microwave images of bio-phantoms simulated using a compact UWB HFMPA model with CF-DMAS beamforming was performed, using the VNA-acquired dielectric data. Benefits: Bandwidth up to 5.71 – 16.94 GHz, peak gain of 5 dB, SAR < 1.6 W/kg [20]. Drawbacks: moderate gain, phantom-only validation, and dependence on the accuracy of the preprocessing. such as feed offsets, substrate height, and ground dimensions were optimized by the ECU-GWO algorithm [21]. Obtained higher gain and directivity along with a lowest convergence cost value of 0.2872 compared to conventional methods.

UWB operation of Compact FR-4 based MSCF Slot Array Antenna with DGS array antenna for 5G mm-wave applications using fractal slots and defected ground structure. Achieved a gain of 5.4–6.1 dBi and a return loss (S11) of 41.83 dB, with coverage across various 5G NR bands.The challenges are FR-4 dielectric losses and limited environmental performance validation [22].

A wideband miniaturized Minkowski Koch Snowflake Fractal Compact Monopole Antenna [23] was fabricated on RT /5880 substrate by combining both Minkowski and Koch-snowflake fractals. The measured prototype achieved 88.84% Fractional Bandwidth (FBW), 2.91 dBi gain, and >60.5% efficiency over the frequency range 8.62–22.40 GHz. Low gain, moderate efficiency, and limited practical deployment environments validation.

The 5G mm-wave application was enhanced with RSGA [24] based Fractal MIMO antenna configuration to get better isolation and multiband resonance. It was fabricated using FR4 substrate and was able to operate from 8 GHz up to 28 GHz with 10.3 GHz isolation below −16 dB and bandwidth. Challenges include FR4 substrate losses, element proximity, and partial band coverage.

To optimize the performance of an E-type plate antenna in terms of dimensional parameters that influence gain and S11 for 5.8 GHz IoT communication, RSM with DoE was used [25]. The measured gain and reflection coefficient were validated experimentally and computed db and dbi, correspondingly. The disadvantages are reduced gain measurement, the difference between the gain measured and the gain obtained, and limited single-band optimization.

To improve the performance of RF harvesting using a conventional patch antenna [26], a 5×5 modified Jerusalem-cross meta surface layer was used, which achieved gain improvement and impedance matching. Experimental test at 2.45 GHz resulted in almost 10 dBi gain enhancement and harvested DC voltage increase. Drawbacks are the narrowband operation, the power decay with distance, and the asymmetric current distribution effects.

A wideband and high-gain 4×4 double-H-shaped slot type MPA array with flexible 1:16 feed network [27] was operated under extreme temperature conditions. As per experimental validation, the bandwidth is 11.4-17 GHz, FBW (39.4%), and 18.7 dBi is recorded at 15.5 GHz. Constraints are: greater array complexity, greater losses in the feed network, and limited compactness in portable applications.

The 28 GHz compact operation of Inset-fed Rectangular Slit Inset-Fed MPA [28] was realized by slit-based size-reduction and impedance optimization on Rogers RT/Duroid-5880 substrate. Simulated validation with HFSS and CST resulted in a return S11 of -45 dB, a bandwidth of 1.43 GHz, above 8 dBi gain, and nearly 99% radiation efficiency. Limitations are single-band focus and simulation-dominated evaluation.

A 2×2 directional fractal antenna array was designed using FR4 and Rogers TMM4 substrates, while a Wilkinson power divider was incorporated to facilitate IEEE 802.11ax and sub-6 GHz 5G communication systems. Fabricated array achieved 85 MHz/4.19 dB bandwidth-gain at 4.17 GHz and 182 MHz/9.61 dB at 5.97 GHz. No losses to substrate dependency, no greater array spacing, and minimal multiband scalability [29].

The tri-wideband wireless communication for WLAN, WiMAX, LTE, and RFID, Bluetooth, and 5G bands was achieved by using a compact Sierpinski hexagonal-shaped TWBA [30]. It was fabricated in a FR-4 substrate and was able to operate in the frequency range from 2.19 GHz to 11.32 GHz and achieved a maximum gain of 4.19 dBi. Some restrictions are moderate gain, losses of the substrate, and limited directional radiation.

3. Materials and Methods

The design, modeling, optimization, and performance enhancement of a small-sized multiband microstrip fractal antenna with the use of DGS techniques for advanced wireless communication applications. The methodology is based on the classical microstrip antenna theory, fractal electromagnetic concepts, ground plane engineering, for improved bandwidth, improved gain, miniaturization, and superior impedance matching. This proposed antenna is based on fractal geometries according to ST and KC models, and triangular DGS slot structures fabricated on an FR4 substrate. Using HFSS Terminal Network excitation, a complete antenna system is modeled and simulated in ANSYS HFSS. Full-wave finite element simulations are performed to conduct parametric optimization, electromagnetic analysis, and performance evaluation. The theoretical antenna calculations, fractal iteration development, DGS integration, numerical simulation, optimization, fabrication planning, and experimental validation are graphically demonstrated by the methodology as shown in Figure 1.

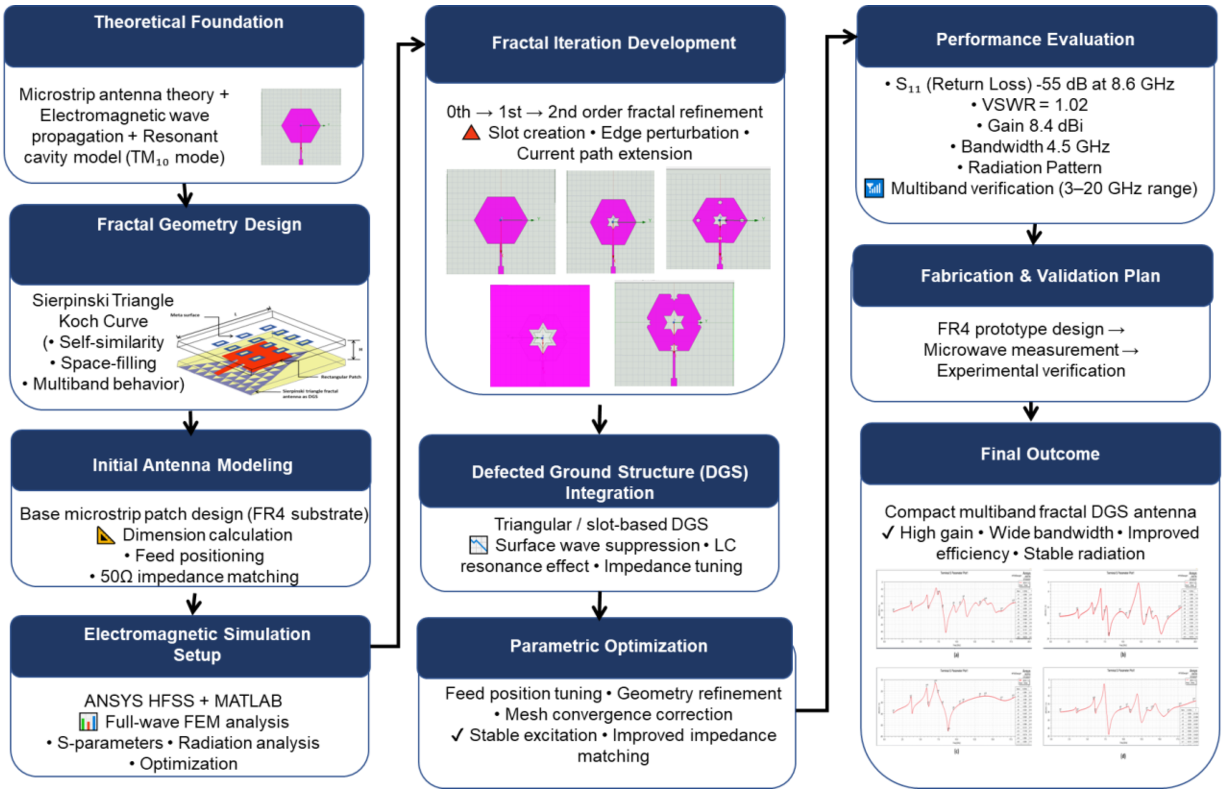

Figure 1: Overall Functional Flow of the Research

3.1 Fundamental Theory of Microstrip Patch Antenna

The design of the proposed antenna is basically a hexagonal MPA, which is a resonant cavity radiator operating in the dominant Transverse Magnetic (TM_{10}) mode. In this mode, the electromagnetic field is mainly confined in the patch length, and the radiation is caused by the fringing electric fields at the radiating edges.

The initial design procedure involves determining the geometrical dimensions of the patch for the target resonant frequency of 2.45 GHz using an FR4 substrate with dielectric constant $\varepsilon_r = 4.4$ and substrate thickness $h = 1.6\ mm$. The patch width W=2mm, which significantly influences radiation efficiency and bandwidth, is calculated as Equation (1).

$$W = \frac{c}{2f_r}\sqrt{\frac{2}{\varepsilon_r+1}} \tag{1}$$

where c represents the speed of light and f_r denotes the resonant frequency. Substituting the design parameters gives $= 38.05\ mm$. Due to fringing field effects, the electromagnetic wave does not remain completely confined within the substrate; therefore, the effective dielectric constant ε_{eff} is introduced and expressed as Equation (2).

$$\varepsilon_{eff} = \frac{\varepsilon_r+1}{2} + \frac{\varepsilon_r-1}{2}\left(1+12\frac{h}{W}\right)^{-1/2} \tag{2}$$

The obtained value is $\varepsilon_{eff} = 4.3986$. h → Height (thickness) of the substrate

W → Width of the microstrip line. Using this parameter, the effective resonant length L_{eff} is calculated as Equation (3).

$$L_{eff} = \frac{c}{2f_r\sqrt{\varepsilon_{eff}}} \tag{3}$$

The fringing field extension $\Delta L$is then evaluated using Equation (4).

$$\Delta L = 0.412h \frac{(\varepsilon_{eff}+0.3)(W/h+0.264)}{(\varepsilon_{eff}-0.258)(W/h+0.8)} \tag{4}$$

Consequently, the actual patch length L becomes expressed in Equation (5).

$$L = L_{eff} - 2\Delta L \tag{5}$$

Which yield is 11.33mm. Furthermore, the ground plane dimensions of length L_g and width W_g are determined using Equations (6 and 7).

$$L_g = L + 6h \tag{6}$$

$$W_g = W + 6h \tag{7}$$

while the feed location coordinates are optimized to achieve proper 50 Ω impedance matching and efficient excitation of the proposed fractal-DGS antenna structure.

3.2 Proposed Fractal Antenna Model

To improve multiband radiation characteristics, miniaturization and impedance bandwidth, the proposed fractal antenna model is developed by integrating fractal-based geometries to the radiating patch structure. Major concepts used in the design are the Sierpinski Triangle and fractal concepts of the Koch type, in which the electromagnetic behavior is highly dependent on self-similarity and iteration of boundary transformations. These geometries are mathematically connected to the eigenvalue problems on a fractal domain, which allows for a rigorous interpretation of the current distribution and resonance formation in the structure of the antenna.

3.2.1 Sierpinski Fractal Geometry (Eigenfunction Interpretation)

The patch is an equilateral patch on which the Sierpinski fractal is created by the recursive removal of the central triangular regions, creating a self-similar structure. Recursive triangular removal and self-similar scaling. Figure 2 illustrates the recursive Sierpinski fractal patch generation process, where central triangular sections are iteratively removed (Figure 2a) to create a self-similar antenna geometry defining the fractal domain. It also presents the boundary field distribution and eigenfunction mapping (Figure 2b), highlighting nodal field potentials with zero-potential edges satisfying Dirichlet boundary conditions for resonance characterization.

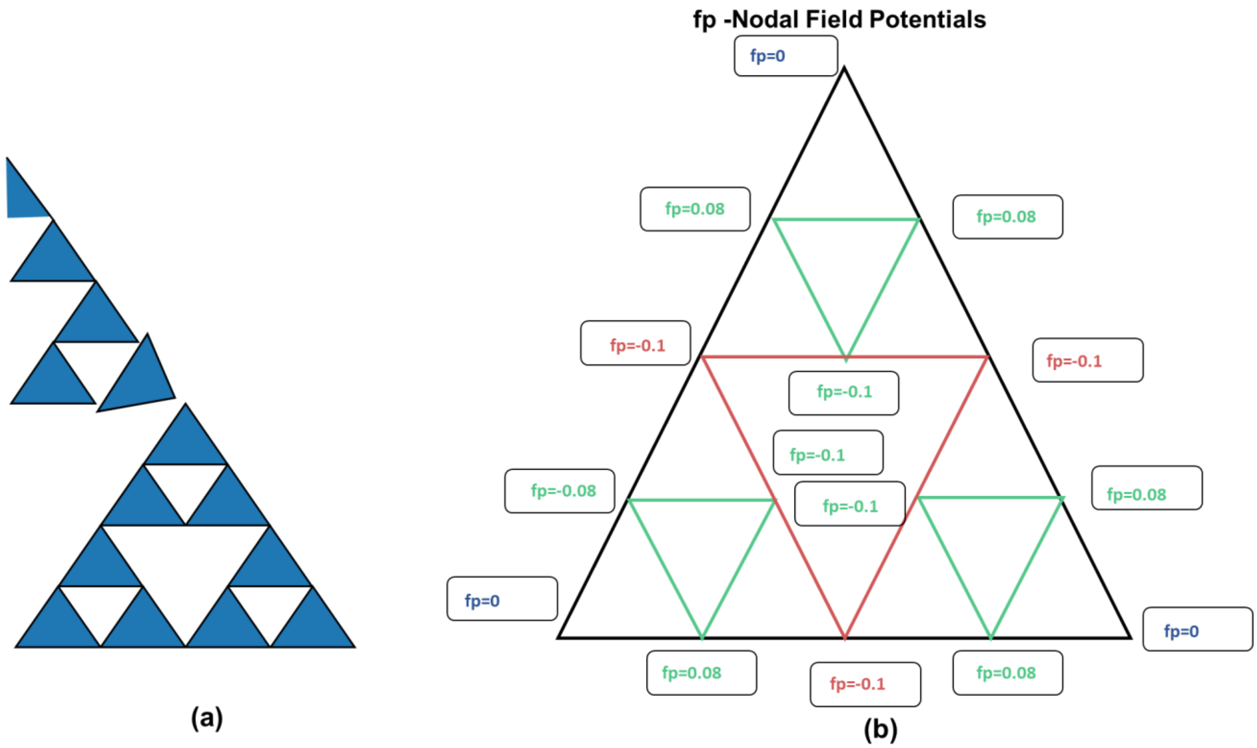

Figure 2: Sierpinski Fractal Patch Geometry (a) Geometric Iteration and Removal and (b) Eigenfunction Distribution

From an electromagnetic perspective, the radiating patch can be modeled as a bounded domain $\Omega \subset \mathbb{R}^2$, where the field distribution satisfies a Helmholtz-type eigenvalue problem is stated in Equation (8).

$$-\Delta u = \lambda u \text{in } \Omega \quad (8)$$

Where $-\Delta$ is the Laplace operator, u represents the electric field distribution (eigenfunction), λ denotes the eigenvalue associated with resonant modes, and Ω is the fractal antenna domain. The Dirichlet boundary condition defines the exact value of the field function along the boundary of the domain, where $u = 0$on $\partial\Omega$, indicating that the electric field remains fixed at the boundary. In contrast, the Neumann boundary condition specifies the value of the normal derivative of the field on the boundary, represented as $\partial u/\partial n=0$,which indicates that no flux passes across the boundary. A Dirichlet model with grounded/zero potential edges is the boundary condition used in antenna analysis, and Neumann corresponds to open or radiation boundary conditions. The numerical computation of the transformation of the continuous domain to a finite mesh is carried out to compute the Eigen values as Equation (9).

$$\mathrm{Lu} = \lambda \mathrm{u} \quad (9)$$

Where L is the discretized Laplacian matrix, $\mathrm{u} \in \mathbb{R}^N$is the nodal field vector, and $N$is the number of discretization points. The Sierpinski iteration introduces a scaling relation is expressed in Equation (10).

$$L_n = \frac{L_0}{2^n} \quad (10)$$

Here, L_0 represents the original patch length, while L_n denotes the effective length obtained after the n^{th} fractal iteration. The fractal dimension can be calculated using Equation (11).

$$D = \frac{\log 3}{\log 2} \approx 1.585 \quad (11)$$

Electromagnetically, this fractal structure generates multiple eigenmodes $\lambda_1, \lambda_2, \lambda_3, \ldots$, which correspond to multiband resonance behavior in the antenna.

3.2.2 Koch Fractal Geometry (Spectral and Eigenvalue Model)

Koch Curve geometry is the second proposed geometry, which is a recursive perturbation of the boundary coupled with an increase in electrical path length. Iterative boundary expansion and increased electrical path length. The fractal boundary leads to modified eigenvalue distribution governed by the Laplacian operator, the spatial energy distribution within the antenna structure $-\Delta u$ as state in Equation (12).

$$-\Delta u = \lambda u \text{ in } \Omega_K \tag{12}$$

where Ω_K denotes the Koch-based fractal domain. The discretized system is similarly expressed as Equation (13).

$$\mathrm{L}_K \mathrm{u} = \lambda \mathrm{u} \tag{13}$$

where L_K represents the Laplacian operator adapted to the Koch boundary.

a. Koch Snowflake Area and Perimeter Evolution

The initial equilateral triangle area A_0 is computed in Equation (14).

$$A_0 = \frac{\sqrt{3}}{4} s^2 \tag{14}$$

Where s is a side length of initial triangle. At each iteration, the additional area A_n is calculated by using the Equation (15).

$$A_n = 3 \cdot 4^{n-1} \cdot \frac{\sqrt{3}}{4} \cdot \frac{s^2}{9^n} \tag{15}$$

Where n is an iteration level/order of the Koch fractal. Thus, the total limiting area A_{total} becomes is stated in Equation (16).

$$A_{\text{total}} = \frac{2\sqrt{3}}{5} s^2 \tag{16}$$

The perimeter grows exponentially as Equation (17).

$$P_n = P_0 \left(\frac{4}{3}\right)^n \tag{17}$$

Where P_0 is an initial perimeter, and P_n denoted as perimeter after n^{th} iteration. This unbounded perimeter growth increases effective current path length, thereby reducing resonant frequency.

3.2.3 Eigenvalue Interpretation of Fractal Antenna Behavior

The electromagnetic response of the proposed fractal antenna is governed by spectral properties of the Laplacian operator. The resonant frequencies are directly related to eigenvalues in Equation (18).

$$f_n = \frac{c}{2\pi} \sqrt{\lambda_n} \tag{18}$$

Where f_n is a resonant frequency of n^{th} mode, $\frac{c}{2\pi}$ denoted as speed of light, and λ_n represented as eigenvalue of fractal domain. The eigenvalue spectrum becomes denser in fractal geometries to boundary irregularity, resulting in multiband and wideband antenna performance.

3.2.4 Electromagnetic Interpretation and Design Contribution

Spectral splitting, the creation of multiple eigenmodes and the increase of effective electrical length without increase in physical length; dense eigenvalue distribution, which provides an improvement of the impedance bandwidth; and the superior miniaturization based on space-filling fractal structure are characteristics that make the integration of Sierpinski and Koch fractal geometries into antennas more effective. From a physical point of view the surface current density satisfies as computed in Equation (19).

$$\nabla \times \mathrm{H} = \mathrm{J} + \frac{\partial \mathrm{D}}{\partial t} \tag{19}$$

Where H is a magnetic field intensity, $\mathrm{J} + \frac{\partial \mathrm{D}}{\partial t}$ signified as current density, and D represented as electric flux density. Fractal antenna model relates the geometry to the electromagnetic eigenvalue theory, and Sierpinski structures provide the discrete multi-resonant modes, and smaller multiband microstrip antennas that are suitable for standard wireless networks can be designed thanks to KC's increased functional length.

3.3 Defected Ground Structure (DGS) Methodology

To suppress the propagation of surface wave and to obtain compact multiband performance for advanced wireless communication systems; DGS is used to get the wide impedance bandwidth. This is done by etching geometry into the metallic ground plane that creates defects, thus changing the distribution of current, and therefore the true inductive and capacitive properties of the transmission structure. The triangular fractal inspired DGS elements proposed using the dumbbell and slot based DGS concepts are used below the radiating patch to increase the electrical path length and to generate more modes for this research.

The multi-layered antenna is a Sierpinski triangle fractal DGS modified current distribution as shown in Figure 3, increases path length, creates parallel LC resonances, and with a metal surface layer, increases the bandwidth, gain, multi-resonant performance, and allows the antenna to be miniaturized.

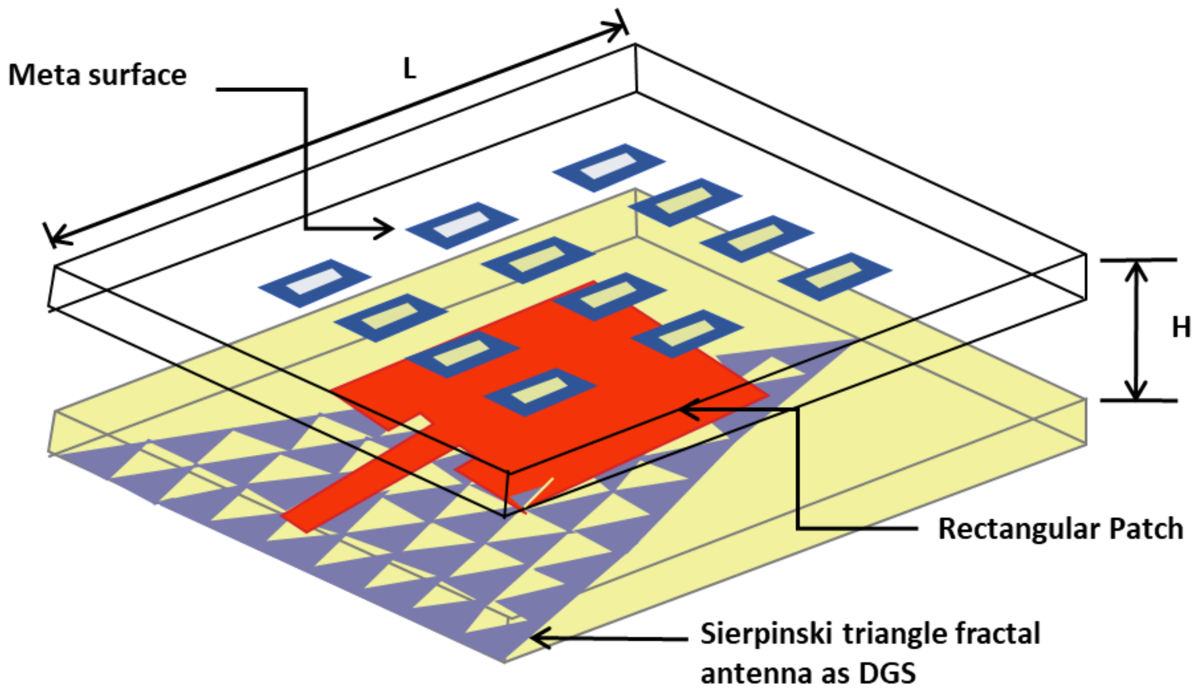

Figure 3: 3D Layered View of the Proposed MPA with Meta surface and Sierpinski Triangle Fractal DGS

The DGS can be considered equivalent to a parallel LC resonator whose resonant frequency is shown in Equation (20), from an electro-magnetic point of view.

$$f_r = \frac{1}{2\pi\sqrt{LC}} \tag{20}$$

Where f_r denoted as resonant frequency of the DGS structure, L represented as equivalent inductance generated by disturbed current path, and $2\pi\sqrt{LC}$ is an equivalent capacitance produced by etched slot discontinuity

DGS has been added to decrease propagation delay, which is beneficial for miniaturization effect but becomes slow wave effect. The propagation constant is denoted as Equation (21).

$$\beta = \omega\sqrt{LC} \tag{21}$$

Where β meant as phase propagation constant, and ω represented as angular frequency. The proposed DGS configuration is similar to a periodic DGS structure, except that the periodic defected geometry is replaced by a single defected geometry, which leads to an improved stop-band behavior and harmonic suppression. The etched triangular slots lead to deeper rejection of defects and to better impedance matching to more concentration of current around the edges of defects. Designed for high slow-wave factor, high compactness, broad operating bandwidth and efficient multi resonant performance, the fractal-triangular DGS is designed to have these advantages. Therefore, the proposed compact microstrip antenna system shows much improvement in the electromagnetic performance with the incorporation of Sierpinski-Koch fractal geometries with DGS.

4. Result and Discussion

The Sierpinski–Koch fractal antenna with DGS shows enhanced multiband performance, impedance matching, gain, and bandwidth, confirming improved radiation characteristics for advanced wireless communication applications compared to conventional designs in literature. The software and hardware setup for Computer-Aided Design (CAD) design, modeling, and simulation of the fractal DGS microstrip antenna, validated virtually with MATLAB and ANSYS HFSS, and the detailed configuration is presented in Table 1.

Table 1: Computational Experimental Design Configuration

Category	Experimental Tools / Setup
Software Tools	MATLAB for fractal geometry modeling, ANSYS HFSS for electromagnetic simulation, parametric optimization, S-parameter, VSWR, gain, bandwidth, and radiation analysis
Hardware Configuration	Intel i7/Ryzen 7 processor, 16 GB RAM, GPU-supported workstation, FR4 substrate material database, HFSS Terminal Network excitation setup for CAD-based antenna modeling and virtual experimental validation

With successive fractal and DGS design modifications, the simulated S_{11} characteristics of the proposed fractal MPA integrated with DGS, as shown in Figure 4, illustrate the gradual improvement of its multiband resonance behavior, impedance matching performance, reduction in return loss, and improvement in operating bandwidth.

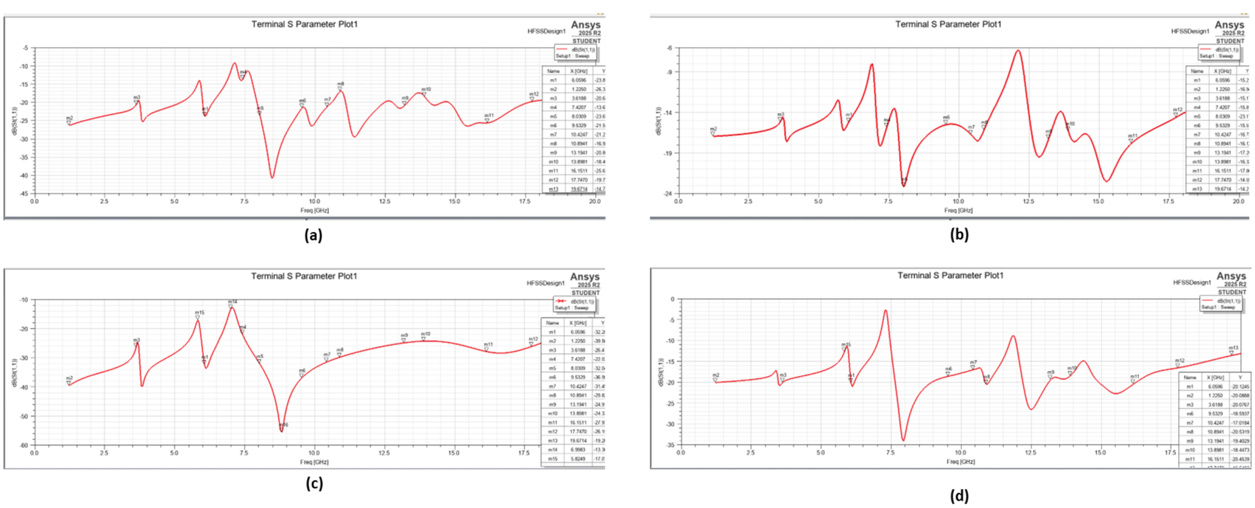

Figure 4: HFSS Simulated Multiband Fractal DGS Antenna Characteristics (a) Initial Resonance, (b) DGS Enhancement, (c) Optimized Matching, and (d) Stable Multiband

As shown in Figure 4(a), the initial fractal antenna response has multiple resonant frequencies at 3.5 GHz, 8.5 GHz, and 13.5 GHz with above 10 resonance markers (m_1–m_{13}) spread across the frequency spectrum, suggesting the self-similar and space-filling behavior of the Sierpinski Triangle and Koch Curve geometries, but a few resonances are close to the standard -10 dB impedance threshold, which requires further optimisation. The HFSS message manager also specifies poor mesh convergence and port integration warnings, indicating mesh refinement and instability in the excitations at higher frequencies. Figure 4(b) shows the effect of the incorporation of the DGS, the resonance at the vicinity of 8.5 GHz deepens considerably below -25 dB which means the matching between the impedances is improved by modifying the distribution of currents on the ground-plane and adding equivalent LC resonance behavior. The antenna also has high-order resonances at frequencies of 10-20 GHz, making it suitable for wideband and satellite-band applications. Optimized configuration in Figure 4(c) with a highly improved resonance near 8.8 GHz (S_{11}-40 dB corresponding to nearly 99.9% power acceptance with low reflection loss) and a wider -10 dB impedance bandwidth than the conventional microstrip antenna. Lastly, the final antenna response of the stabilized final antenna that retains distinct multiband resonances at 3.8 GHz, 8.5 GHz and 11-15 GHz is demonstrated in Figure 4(d), which is compatible with WLAN, WiMAX, radar, and satellite communication systems. In the analysis of the results, stable adaptive meshing, proper port excitation and accurate electromagnetic convergence were confirmed with successful Normal completion of the simulation message, which means that the proposed fractal-DGS antenna design is effective for compact multiband wireless communication applications.

The optimized antenna shows a significant enhancement in the antenna presentation parameters from the projected fractal patch array antenna integrated with DGS as shown from the HFSS simulation plots. The minimum return loss (S11) obtained was about −55 dB at 8.6 GHz, which was good enough to show that excellent impedance matching had been obtained. Multiband characteristics were confirmed with multiple resonant bands observed within 3 GHz – 20 GHz frequency range. The VSWR values were less than 2 at the main resonant frequencies, and the lowest VSWR was around 1.02, guaranteeing an effective power transfer. The antenna exhibited an increased impedance bandwidth of almost 4.5 GHz which encompassed the important wireless communication bands. The simulated gain

of the antenna was about 8.4 dBi and the radiation pattern had stable directional characteristics with the radiation efficiency increased and the back lobe radiation decreased to the use of DGS.

The proposed fractal design of Narrow band to Compact Multiband High Performance MPA integrated with DGS is geometrically progressed with ANSYS 3D Modeler, as shown in Figure 5. This design evolves from a conventional narrowband radiator, to a compact, high performance multiband MPA, offering improved bandwidth utilization, impedance matching, and effective miniaturization for multiband operation.

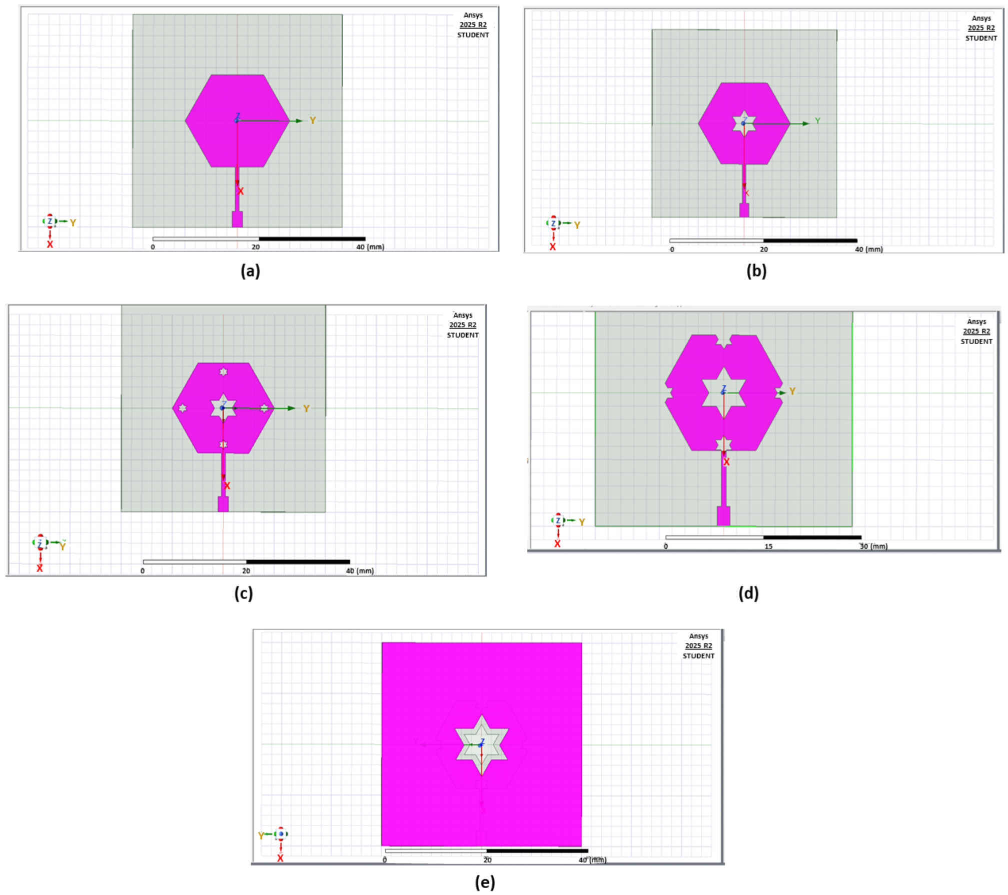

Figure 5: Evolutionary Fractal DGS Antenna Design Methodology Process (a) Base Patch, (b) Initial Fractal, (c) Fractal Refinement, (d) Boundary Fractal, and (e) DGS Integration

Figure 5(a) depicts the initial conventional hexagonal MPA fabricated on an FR4 epoxy substrate with a microstrip feed line, where the radiating element supports a dominant single resonant mode characteristic of conventional microstrip structures, thereby exhibiting limited impedance bandwidth and single-band behavior. Figure 5(b) illustrates the first-order fractal modification in which a centralized star-shaped or Sierpinski-inspired triangular slot is etched into the radiating patch. Self-similarity is introduced and the electrical path length is efficiently augmented without amplify in physical size, thus changing the resonances towards low frequencies and enabling multiband behavior. Figure 5(c) shows the second-order fractal design where extra slots and edge notches are introduced on the perimeter of the hexagonal radiator. Space filling results in fragmented current flow paths with multiple resonant paths of different electrical lengths and improves the multiband resonant behavior via better coupling of the adjacent resonant modes. In Figure 5(d), the optimized antenna design which incorporates triangular fractalization or Koch fractalization at the boundaries along with DGS is shown. In Figure 5(e), the optimized back side ground plane design with the DGS is illustrated where the fractalized slot cut is introduced in the back side ground plane under the radiating element. The DGS modifies the return current distribution and introduces equivalent inductive-capacitive (LC)loading behavior, thereby suppressing surface-wave propagation, compensating reactive impedance, reducing reflection loss, and significantly enhancing S_{11}, gain, and radiation efficiency. Collectively, this validates the progressive transformation of a conventional narrow-band patch antenna into a compact multiband fractal-DGS antenna suitable for WLAN, WiMAX, IoT, radar, and satellite communication applications.

Figure 6 depicts the 2D polar radiation pattern for the fractal DGS micro strip patch antenna simulated by HFSS. The broadside radiation characteristics of this antenna are illustrated through the maximum radiation occurring at 0°, meaning that the radiation is predominantly toward the front, while any backward radiation is suppressed. This antenna demonstrates stable multi trace operation because of its multi-resonance property, thanks to the Sierpinski-Koch fractal structure.

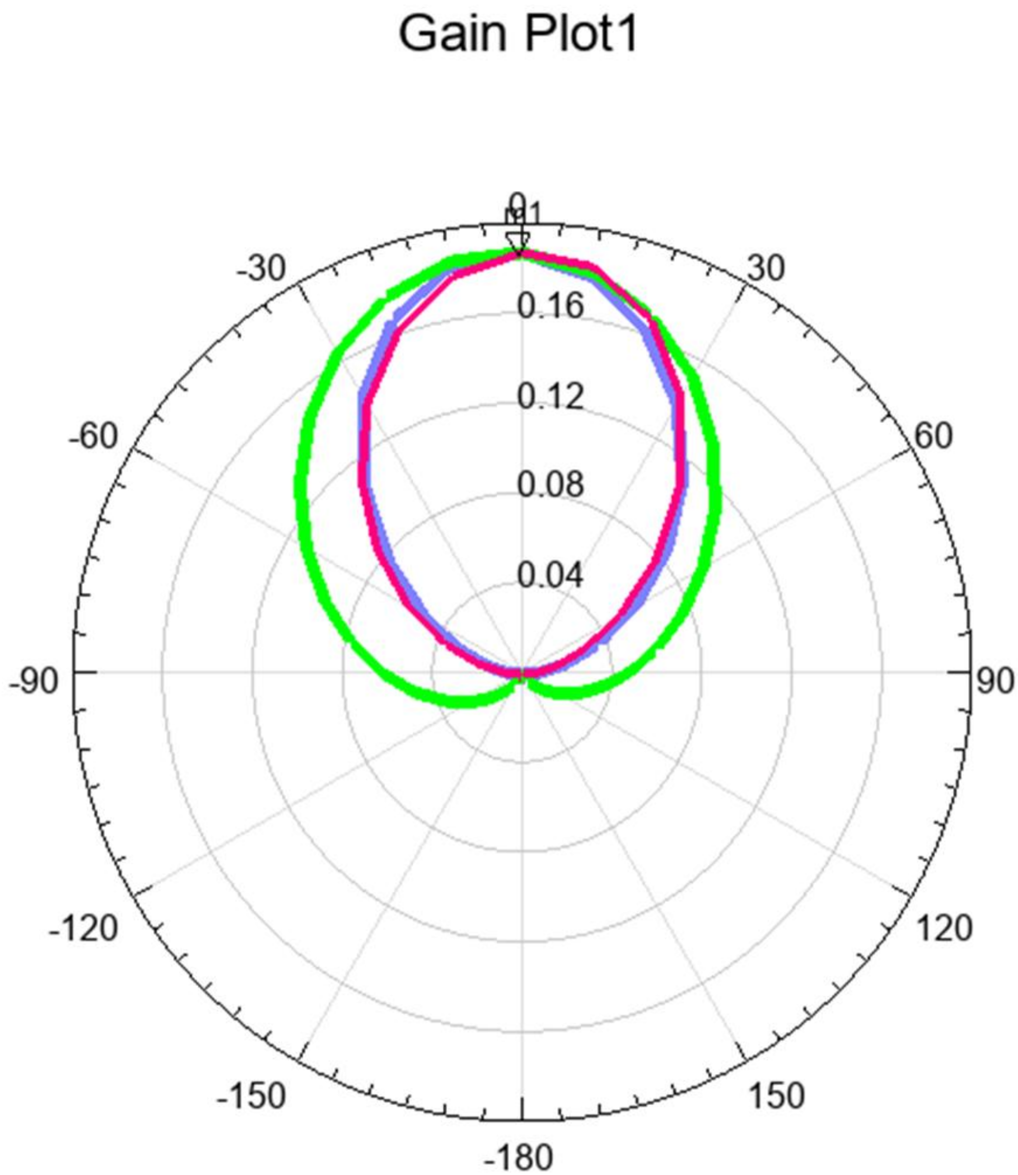

Figure 6: Radiation Pattern of the Proposed Fractal DGS Microstrip Patch Antenna

The performance evolution of the proposed fractal patch antenna for successive designs in quantitative form. Table 2 lists the progressive geometric modification and the ultimate integration of the DGS with the gain, return loss (S11), and impedance bandwidth improvements, which clearly shows the effectiveness of the iterative design approach.

Table 2: Performance Evolution of Fractal Patch Antenna with DGS

Iteration	Structure Description	Gain (dB)	S11 (dB)	Bandwidth (GHz)
(1)	Basic hexagonal patch	3.2	-18.5	1.2
(2)	Hexagonal patch with central slot	5.6	-32.4	2.8
(3)	Multi-slot modified patch	6.9	-41.7	3.6
(4)	Optimized fractal patch array with DGS	8.4	-55.0	4.5

The optimized Star Slot DGS uses a length of 12 mm, width of 5 mm, slot depth of 2.0 mm and a ground plane of 40 mm × 40 mm. These dimensions not only change the ground current distribution, but also suppress the propagation of surface waves, enhance the impedance matching, and result in better gain, bandwidth and return loss of the proposed fractal patch antenna. A detailed geometry and dimensional parameters of the optimized Star Slot DGS is shown in Figure 7.

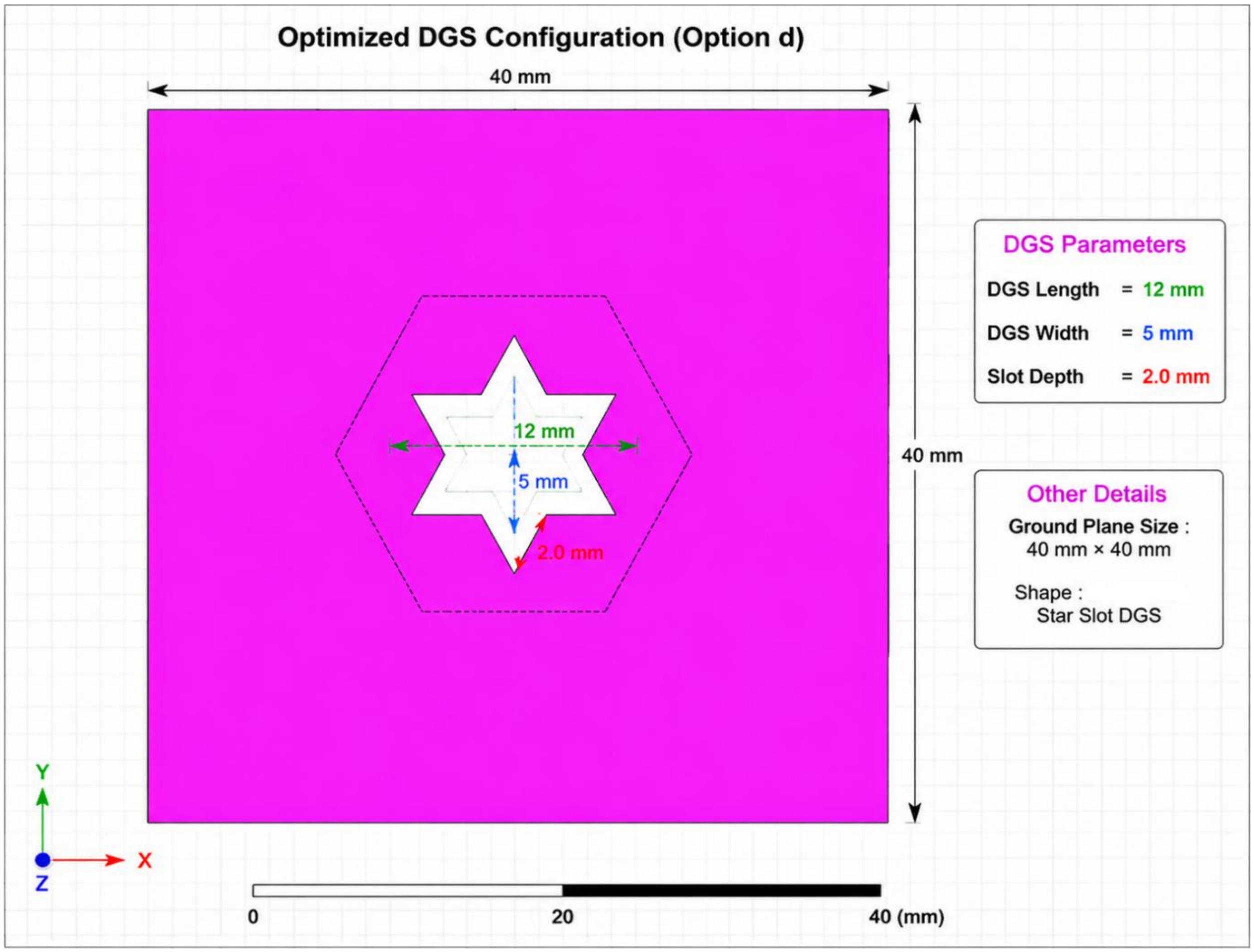

Figure 7: Optimized Star Slot DGS Geometry Parameters

Comparative Evaluation

The comparison between existing literature studies and the proposed study reveals that there have been major developments in the field of fractal antenna and microstrip antenna design in various fields such as 5G technology, MIMO systems, radio-frequency energy harvesting, internet of things, and biomedical imaging, where most existing literature has successfully achieved wideband performance, moderate gain, or improved isolation but is still hindered by problems such as substrate losses, limited gain improvement, single band operation, and lack of real-time testing. Table 3 provides a comparison of existing fractal and microstrip antennas and The proposed antenna

Table 3: Comparative Performance Evaluation of Fractal and Micro-strip Antenna Systems

Ref	Model / Domain	Bandwidth / Frequency Range	Gain	Return Loss / Reflection Coefficient	Other Numerical Results
[20]	UWB HFMPA / Microwave Breast & Forearm Imaging	5.71-16.94 GHz	5 dB	-	SAR < 1.6 W/kg
[21]	ECU-GWO Optimized Fractal Antenna / Antenna Optimization	-	-	-	Cost convergence = 0.2872
[22]	Modified Sierpinski Carpet Fractal Slot Array / 5G mm-Wave	n257, n258, n260, n261	5.4-6.1 dBi	41.83 dB	-
[23]	Minkowski Koch Snowflake Fractal Monopole / Wideband Antenna	8.62–22.40 GHz	2.91 dBi	-	88.84% FBW, >60.5% efficiency
[24]	Fractal Spherical-Slot MIMO Antenna / 5G mm-Wave	8–28 GHz	-	Isolation < -16 dB	10.3 GHz bandwidth
[25]	DOE-RSM E-Type Plate Antenna / IoT Communication	5.8 GHz	2.65 dBi	11.2 dB	-
[26]	Jerusalem-Cross Meta Surface Patch Antenna / RF Energy Harvesting	2.45 GHz	~10 dBi	-	-
[27]	Double-H-Shaped Slot Patch Array / Wideband High-Gain Array	11.4-17 GHz	18.7 dBi	-	39.4% FBW
[28]	Inset-Fed Rectangular Slit Patch Antenna / 28 GHz Communication	28 GHz	>8 dBi	-45 dB	1.43 GHz bandwidth, ~99% efficiency
[29]	Minkowski-Sierpinski Fractal Array / IEEE 802.11ax & Sub-6 GHz 5G	4.17 GHz / 5.97 GHz	4.19 dB / 9.61 dB	-	85 MHz / 182 MHz bandwidth
[30]	Sierpinski Hexagonal Tri-Wideband Fractal Antenna / WLAN, WiMAX, LTE, RFID, 5G	2.19-11.32 GHz	4.19 dBi	-	-
[Proposed]	Sierpinski–Koch Fractal DGS Patch Array Antenna / Multiband Wireless Communication	3-20 GHz	8.4dBi	-55 dB at 8.6 GHz	VSWR = 1.02, 4.5 GHz bandwidth, multiband resonance, improved radiation efficiency

design was evaluated based on key performance parameters, including bandwidth, gain, return loss, efficiency, and its suitability for various application domains.

The proposed Sierpinki–Koch fractal DGS antenna overcomes the main drawbacks of existing literature by combining both multiband fractal geometry and DGS technique to achieve high level of impedance matching, high radiation efficiency, high gain performance and wideband operation,

5. Conclusion

A compact wideband microstrip fractal patch antenna with a defected ground structure (DGS) was designed and analysed for wireless communication applications. The combination of the Sierpinski–Koch fractal geometry and the DGS improved the surface current distribution, leading to better impedance matching, wider bandwidth, and stable radiation characteristics while maintaining a compact antenna size.

The simulated performance indicates that the proposed design provides an effective way to enhance the electrical characteristics of a microstrip patch antenna without increasing its overall dimensions. Owing to its compact structure and improved performance, the antenna is suitable for applications such as WLAN, WiMAX, IoT, radar, and satellite communication. Future work will focus on prototype fabrication, experimental validation, the use of low-loss substrate materials, and further optimization to improve antenna performance for next-generation wireless communication systems.

Reference

1. El Issawi, M. L., Konditi, D., & Usman, A. D. (2024). Design of enhanced wide band microstrip patch antenna based on defected ground structures (DGS) for sub-6 GHz applications. International Journal of Electrical and Electronics Research, 12(1), 315-321. https://doi.org/10.37391/IJEER.120143
2. Raj, A., & Mandal, D. (2024). Design and experimental analysis of fractal antennae with ground-defected structure for expected 6G and 5G mm-wave communication and wireless applications. Transactions on Emerging Telecommunications Technologies, 35(1), e4900. https://doi.org/10.1002/ett.4900
3. Ramineni, P., & Nimmala, A. (2024). Design and Analysis of Microstrip Patch Antennas with Polygonal and Rectangular Defected Ground Structures for Sub-6GHz Applications. International Journal of Wireless and Microwave Technologies, 14(5), 44-58. https://doi.org/10.5815/ijwmt.2024.05.04
4. TS, A. S. (2025). Enhancing gain and bandwidth in a multiband microstrip patch antenna through L-slot and partial ground plane integration. Scientific Reports, 15(1), 1-12. https://doi.org/10.1038/s41598-025-13947-8
5. Tewary, T., Maity, S., Roy, A., Mandal, K., Kundu, S., & Bhunia, S. (2024). Design and analysis of frequency selective surface embedded broadband high gain miniaturized antenna. International Journal of Communication Systems, 37(8), e5754. https://doi.org/10.1002/dac.5754
6. Ajewole, B., Kumar, P., & Afullo, T. (2023). A microstrip antenna using I-shaped metamaterial superstrate with enhanced gain for multiband wireless systems. Micromachines, 14(2), 412. https://doi.org/10.3390/mi14020412
7. Armghan, A., Lavadiya, S., Alsharari, M., Aliqab, K., Daher, M. G., & Patel, S. K. (2023). Highly efficient and multiband metamaterial microstrip-based radiating structure design showing high gain performance for wireless communication devices. Crystals, 13(4), 674. https://doi.org/10.3390/cryst13040674
8. Noor, S. K., Jusoh, M., Sabapathy, T., Rambe, A. H., Vettikalladi, H., M. Albishi, A., &Himdi, M. (2023). A patch antenna with enhanced gain and bandwidth for sub-6 GHz and sub-7 GHz 5G wireless applications. Electronics, 12(12), 2555. https://doi.org/10.3390/electronics12122555
9. Khan, H., Ullah, H., Mazhar, S. A. I., Hassan, M., & Farooq, I. (2024). Miniaturization of Microstrip Patch Antenna Using Fractal Geometry. International Journal of Advanced Networking and Applications, 16(3), 6374-6381. https://doi.org/10.35444/IJANA.2024.16301
10. Kim, J., Keun, J., Yoo, T., & Lim, S. (2023). Miniaturization and bandwidth enhancement of fractal-structured two-arm sinuous antenna using gap loading with meandering. Fractal and Fractional, 7(12), 841. https://doi.org/10.3390/fractalfract7120841
11. Sanu, S. V., Rodrigues, S., Vallikkunnel, J. K. N., & Sivan, S. A. (2023). Fractal-enhanced microstrip antennas: miniaturization, multiband performance and cross-polarization minimization for Wi-Fi applications. Engineering Proceedings, 59(1), 127. https://doi.org/10.3390/engproc2023059127
12. Patel, S. K., & Baz, A. (2023). O-shape fractal antenna optimized design with broad bandwidth and high gain for 6G mobile communication devices. Fractal and Fractional, 8(1), 17. https://doi.org/10.3390/fractalfract8010017
13. Verma, A., Patil, S., Singh, A. K., & Pandey, A. K. (2023). Notched circular EBG based circularly polarized antenna for performance enhancement. Journal of Microwaves, Optoelectronics and Electromagnetic Applications, 22(1), 47-62. https://doi.org/10.1590/2179-10742023v22i1265710
14. Chang, W., Chen, S., Chen, K., Yu, P., & Liu, Q. H. (2024). Mutual coupling reduction in antenna arrays using the novel mushroom electromagnetic band gap and defected ground structure. Microwave and Optical Technology Letters, 66(2), e34084. https://doi.org/10.1002/mop.34084
15. Viet, D. N. T., Tran-Huy, H., Quoc, D. N., & Park, H. C. (2024). A novel defected ground structure for high-isolation circularly polarized MIMO patch antenna. Journal of Electromagnetic Waves and Applications, 38(1), 34-48. https://doi.org/10.1080/09205071.2023.2270524
16. Roja, G., Venkatesh, P. M., & Jayasankar, T. (2025). Design and Optimization of a Pentaband Offset Feed Closed Ring Resonator Antenna for Wireless Applications. Tehničkivjesnik, 32(6), 2199-2204. https://doi.org/10.17559/TV-20241231002224
17. Alhaj Hasan, A., Nguyen, T. M., Kuksenko, S. P., &Gazizov, T. R. (2023). Wire-grid and sparse MoM antennas: Past evolution, present implementation, and future possibilities. Symmetry, 15(2), 378. https://doi.org/10.3390/sym15020378
18. Ullah, K., Khan, W., Aziz, A., Zeb, M., Yousaf, M. Z., Altayeb, M., &Bereznychenko, V. (2026). Design, Simulation, and Optimization of Cavity Patch Antenna used in Next-Generation 5G Wireless Communication. Int. J. Advanced Networking and Applications, 17(04), 7008-7022. https://doi.org/10.35444/IJANA.2025.17403
19. Cao, Z., & Lu, M. (2025). Advancements in Wearable Antenna Design: A Comprehensive Review of Materials, Fabrication Techniques, and Future Trends in Wireless Communication. Micromachines, 16(9), 1028. https://doi.org/10.3390/mi16091028

20. Kaur, K., & Kaur, A. (2025). A hybrid fractal microstrip patch antenna rooted from pythagoras-koch snowflake geometries for microwave imaging of skin and breast cancer. Physica Scripta, 100(8), 085547.https://doi.org/10.1088/1402-4896/adf7de
21. Reddy, S. K., &Guttavelli, A. (2025). Designing of optimized microstrip fractal antenna using hybrid metaheuristic framework for IoT applications. Journal of Systems Engineering and Electronics, 36(3), 659-670. https://doi.org/10.23919/JSEE.2024.000115
22. Raj, A., & Mandal, D. (2025). Design and performance analysis of fractal slot array antenna for advanced 5G mm-wave applications. International Journal of Electronics, 112(8), 1821-1843. https://doi.org/10.1080/00207217.2024.2408788
23. Sood, M., & Rai, A. (2023). Design of compact fractal patch antenna for X/Ku/K-band applications. International Journal of Communication Systems, 36(11), e5515. https://doi.org/10.1002/dac.5515
24. Bisht, N., Malik, P. K., Das, S., Islam, T., Asha, S., &Alathbah, M. (2023). Design of a modified MIMO antenna based on tweaked spherical fractal geometry for 5G new radio (NR) band N258 (24.25–27.25 GHz) applications. Fractal and Fractional, 7(10), 718. https://doi.org/10.3390/fractalfract7100718
25. Chen, J. H., Cheng, C. Y., Chien, C. M., Yuangyai, C., Chen, T. H., & Chen, S. T. (2023). Multiple performance optimization for microstrip patch antenna improvement. Sensors, 23(9), 4278. https://doi.org/10.3390/s23094278
26. Almizan, H., Jwair, M. H., Al Naiemy, Y., Hassain, Z. A. A., Nagy, L., & Elwi, T. A. (2023). Novel metasurface based microstrip antenna design for gain enhancement RF harvesting. Infocommunications Journal, 15(1), 2-8. https://doi.org/10.36244/ICJ.2023.1.1
27. Li, R., Li, P., Rocca, P., Salas Sánchez, A. Á., Song, L., Li, X., ... & Fan, Z. (2023). Design of wideband high-gain patch antenna array for high-temperature applications. Sensors, 23(8), 3821. https://doi.org/10.3390/s23083821
28. Gaid, A. S., Ali, M. A., Saif, A., & Mohammed, W. A. (2024). Design and analysis of a low profile, high gain rectangular microstrip patch antenna for 28 GHz applications. Cogent Engineering, 11(1), 2322827. https://doi.org/10.1080/23311916.2024.2322827
29. Vallappil, A. K., Khawaja, B. A., Rahim, M. K. A., Uzair, M., Jamil, M., & Awais, Q. (2023). Minkowski–Sierpinski fractal structure-inspired 2× 2 antenna array for use in next-generation wireless systems. fractal and fractional, 7(2), 158. https://doi.org/10.3390/fractalfract7020158
30. Benkhadda, O., Saih, M., Ahmad, S., Al-Gburi, A. J. A., Zakaria, Z., Chaji, K., & Reha, A. (2023). A miniaturized tri-wideband sierpinski hexagonal-shaped fractal antenna for wireless communication applications. Fractal and Fractional, 7(2), 115. https://doi.org/10.3390/fractalfract7020115